

Generation of neutron multigroup constants in the energy range 0.1 μeV –10 MeV for light and heavy water at four different temperatures

Yoshinobu Edura*, Nobuhiro Morishima

Department of Nuclear Engineering, Kyoto University, Yoshida, Sakyo-ku, Kyoto 606-8501, Japan

Received 20 July 2005; received in revised form 16 October 2005; accepted 9 January 2006

Available online 3 February 2006

Abstract

On the basis of the cross section models of neutron scattering in liquid H_2O and D_2O , which have been developed in the previous papers, we have generated eight sets of multigroup constants (energy-averaged cross sections) for each liquid at 5, 27, 52 and 77 °C. The multigroup constants cover a wide energy range 0.1 μeV –10 MeV with 140 energy groups at equal logarithmic intervals and represent an angular scattering distribution by the Legendre polynomial expansion up to order 3. Major characteristics of neutron scattering inherent to liquid water are fully included in terms of coherent and incoherent properties and temperature-dependent quasi-elastic and inelastic scattering. These characteristics are assured by comparison with relevant experimental results of scattering cross section and also by neutron slowing-down and thermalization analysis in liquid H_2O and D_2O . It is shown that the present multigroup constants serve for analysis of neutron moderation from fission/spallation to ultra-cold energies, in combination with the already-generated ones for liquid ^4He , H_2 , D_2 and CH_4 and solid CH_4 .

© 2006 Elsevier B.V. All rights reserved.

PACS: 61.25.Em; 78.70.Nx; 28.20.Gd; 29.25.Dz

Keywords: Light water; Heavy water; Neutron cross section; Neutron source; Group constant; Neutron transport

1. Introduction

During the past 3 years an extensive study of neutron scattering in liquid water has been carried out with a view to developing a cross section model [1–4].

- Cold and thermal neutron scattering in liquid H_2O has been studied in terms of a physical cross section model expressed basically by a velocity auto-correlation function and, equivalently, a generalized frequency distribution. The microscopic dynamics of water molecules is fully described from very general considerations connected with jump diffusion, intermolecular vibration, hindered rotation and intramolecular vibration at temperatures between 0 and 100 °C.
- The cross section model has been generalized to the one of liquid D_2O . Coherent neutron scattering is treated in view

of a microscopic static structure and molecular motions through the Vineyard's convolution approximation [5]: a set of partial static structure factors for pairs of DD, DO and OO, determined experimentally [6], is utilized to express interference scattering from distinct molecules.

- A full set of double-differential and total cross sections for neutron incident energies from 0.1 μeV (ultra-cold) to 10 eV (epi-thermal) has become numerically calculable. Satisfactory agreement with the neutron scattering experiments and computer simulations [7–19] has been shown at several different temperatures. For reference, such a typical example is given in Fig. 1 for scattering laws for liquid H_2O and D_2O . Inclusion of water molecule dynamics well reproduces the experimentally observed behavior [14–16,20] especially at small momentum and energy transfer, which is in contrast to the molecular gas models for H_2O [21] and D_2O [22].

In the present paper, eight sets of multigroup constants (energy-averaged cross sections) for liquid H_2O and D_2O at

*Corresponding author. Tel.: +81 75 753 5836; fax: +81 75 753 5836.
E-mail address: edura@nucleng.kyoto-u.ac.jp (Y. Edura).

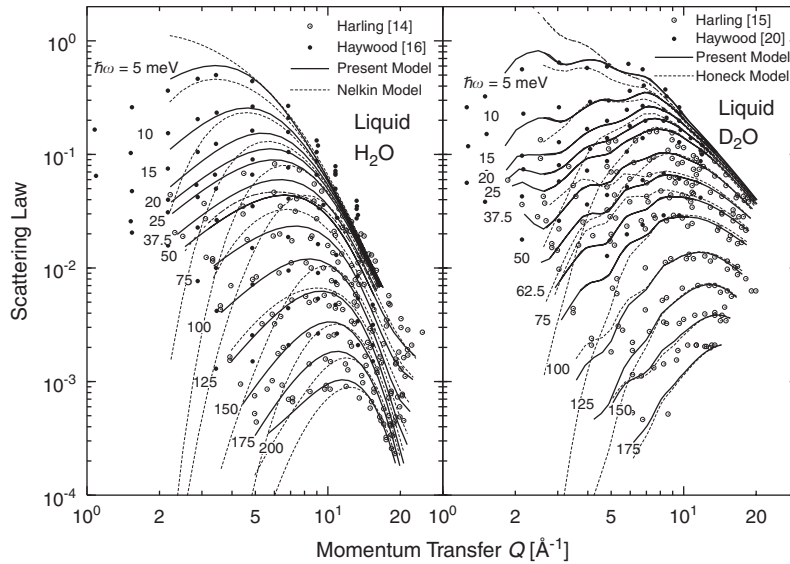


Fig. 1. Calculated scattering laws as a function of energy transfer $\hbar\omega$ and momentum transfer Q for liquid H_2O and D_2O at 20°C , compared with the experimental results [14–16,20] and the Nelkin and Honeck models [21,22].

5, 27, 52 and 77°C are newly generated using the cross section model mentioned above. A wide range of neutron energies from $0.1\ \mu\text{eV}$ to $10\ \text{MeV}$ is covered and forward scattering inherent to H by epi-thermal and fast neutrons is adequately represented by the Legendre polynomial expansion up to order 3. By the combined use of the already-developed multigroup constants for liquid H_2 and D_2 [23], liquid and solid CH_4 [24], and liquid ^4He [25], it becomes possible to treat quantitatively neutron slowing down and thermalization over the extremely wide energy range, say, from fission/spallation to ultra-cold-neutron energies. All the sets of multigroup constants are expected to serve for research and development of an advanced neutron source.

The purpose of the present paper is to report that the newly generated multigroup constants exhibit not only all of the essential characteristics of liquid water dynamics, but also yield proper energy spectra of fast and thermal neutron fluxes inherent to liquid H_2O and D_2O . The former is assured by calculating group-transfer scattering cross sections, angular distributions of scattered neutrons and total scattering cross sections especially at low energies below $10\ \text{eV}$. Good agreement with many experimental results [14,15,17,19,26–29] is found, for instance, with respect to the temperature dependence of total scattering cross sections at very-cold neutron energies around $0.01\ \text{meV}$. The latter spectral analysis is performed by a multigroup neutron transport calculation for pure liquid H_2O and D_2O and their mixtures at each temperature. The thermal neutron spectra are compared with the experimental ones in water and aqueous boric acid solutions [29] and characterized in terms of effective neutron temperature and thermal neutron gain with a change in liquid temperature and $\text{H}_2\text{O}/\text{D}_2\text{O}$ content. Furthermore, non-Maxwellian deviations of the calculated spectra are found and clarified in view of water molecular dynamics such as

quasi-elastic scattering and hindered rotation, which is essentially in contrast to the molecular gas models [21,22].

Section 2 describes briefly the procedures of multigroup constant generation. Section 3 illustrates physical characteristics of the multigroup constants. Section 4 is devoted to the concluding remarks.

2. Generation of multigroup constants

Since the method and procedure of multigroup constant generation have been described [30], only the main points concerned hereupon are touched. The energy range of incident and scattered neutrons from $0.1\ \mu\text{eV}$ to $10\ \text{MeV}$ is divided at equal logarithmic intervals into 140 groups: total number of groups is $G = 140$ with 10 groups per one energy decade. The angular distribution of scattering cross section is represented by the Legendre polynomial expansion up to a maximum order $L = 3$, i.e. in the P_3 approximation, which is almost adequate for reproducing forward scattering in free H, D and O by epi-thermal and fast neutrons. Hence the multigroup constants are defined using the double-differential scattering cross section $d^2\sigma_s^X(E \rightarrow E', \theta)/d\Omega dE'$ for liquid H_2O and D_2O ($X = \text{H}_2\text{O}$ or D_2O) at scattering angle θ with the change of neutron energy from E to E' :

$$\sigma_{s,g \rightarrow g'}^{l,X} = 2\pi \int_{-1}^1 d\mu \int_{E_g}^{E_{g-1}} dE \int_{E_{g'}}^{E_{g'-1}} dE' \times w(E) \frac{d^2\sigma_s^X(E \rightarrow E', \theta)}{d\Omega dE'} P_l(\mu) \quad (1)$$

where $\mu = \cos\theta$, $P_l(\mu)$ is the Legendre polynomial function of order l ($= 0, 1, 2, 3$), E_g and E_{g-1} are the lower and upper boundaries of the energy group g ($g = 1, 2, 3, \dots, G$), and $w(E)$ is the weighting spectrum of neutron flux consisting of

Maxwellian flux, $1/E$ component and fission spectrum with $\int_{E_g}^{E_{g-1}} w(E) dE = 1$.

The total cross sections for scattering and absorption in group g are written as

$$\sigma_{s,g}^X = \sum_{g'=1}^G \sigma_{s,g \rightarrow g'}^{0,X} \quad (2)$$

$$\sigma_{a,g}^X = \int_{E_g}^{E_{g-1}} dE w(E) \sigma_a^X(E) \quad (3)$$

where $\sigma_a^X(E) = \sigma_{a0}^X \sqrt{E_0/E}$ with $\sigma_{a0}^{\text{H}_2\text{O}} = 6.652 \times 10^{-1} \text{ b/H}_2\text{O}$ and $\sigma_{a0}^{\text{D}_2\text{O}} = 1.038 \times 10^{-3} \text{ b/D}_2\text{O}$ at thermal neutron energy $E_0 = 25 \text{ meV}$ [19]. Hence the total cross section for any type of reaction is just

$$\sigma_{t,g}^X = \sigma_{s,g}^X + \sigma_{a,g}^X.$$

Notice that the macroscopic cross sections can be defined as

$$\begin{aligned} \Sigma_{s,g \rightarrow g'}^{l,X} &= N \sigma_{s,g \rightarrow g'}^{l,X}, & \Sigma_{s,g}^X &= N \sigma_{s,g}^X \\ \Sigma_{a,g}^X &= N \sigma_{a,g}^X & \text{and} & \quad \Sigma_{t,g}^X = N \sigma_{t,g}^X \end{aligned}$$

where N is the number density of molecules being common to both liquids [31]: $N/10^{24} = 0.03345, 0.03333, 0.03303$ and 0.03257 cm^{-3} at 5, 27, 52 and 77 °C, respectively.

3. Physical characteristics of multigroup constants

3.1. Inelastic and quasi-elastic scattering processes

Various scattering processes in the whole energy region may be conveniently represented by $\sigma_{s,g \rightarrow g'}^{0,X}$, called the group-transfer scattering cross section. It represents all the scattering processes connected with the change of neutron energy group from g to g' , but being irrelevant to θ as an isotropic ($l = 0$) component.

Figs. 2 and 3 show, respectively, $\sigma_{s,g \rightarrow g'}^{0,\text{H}_2\text{O}}$ and $\sigma_{s,g \rightarrow g'}^{0,\text{D}_2\text{O}}$ at 5 and 77 °C, in which the histograms are plotted as a function of $E = \sqrt{E_g E_{g-1}}$ and $E' = \sqrt{E_{g'} E_{g'-1}}$ in the range of E and $E' \leq 10 \text{ eV}$ (i.e. g and $g' \geq 60$). The following scattering processes can be seen from Figs. 2 and 3: (a) the sharp peaks of quasi-elastic scattering along the diagonal line $E \sim E'$ are obvious. They arise from the translational diffusion of water

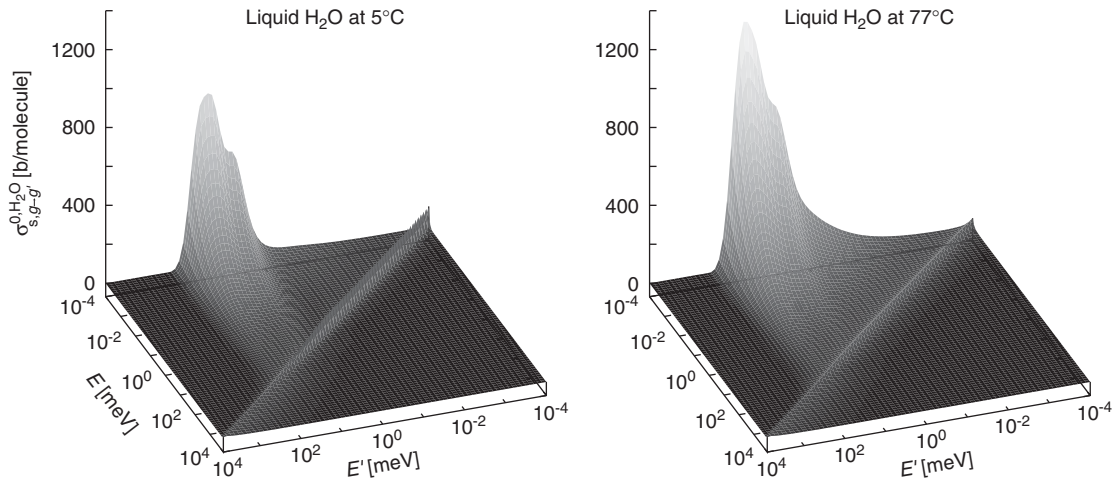


Fig. 2. Group transfer cross sections $\sigma_{s,g \rightarrow g'}^{0,\text{H}_2\text{O}}$ from $E = \sqrt{E_g E_{g-1}}$ to $E' = \sqrt{E_{g'} E_{g'-1}}$.

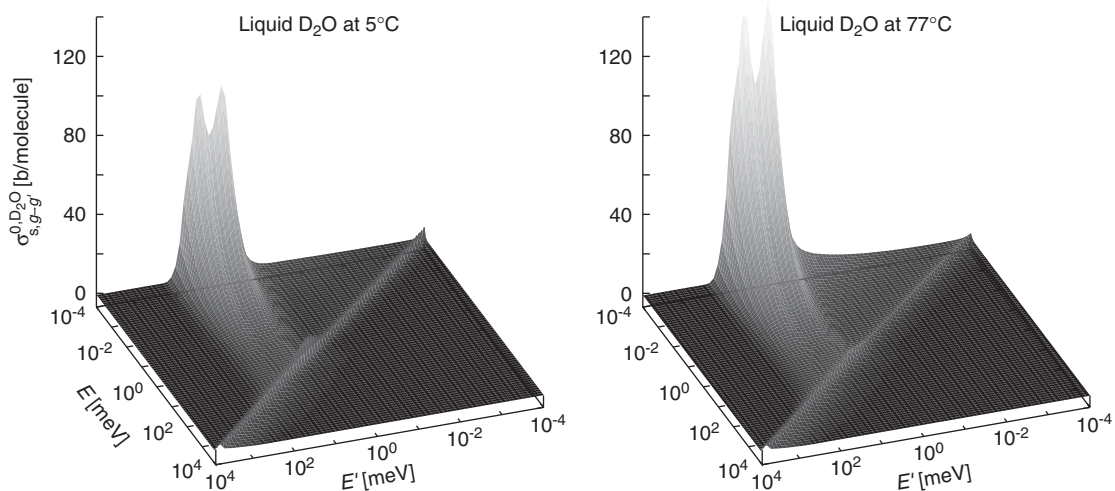


Fig. 3. Group transfer cross sections $\sigma_{s,g \rightarrow g'}^{0,\text{D}_2\text{O}}$ from $E = \sqrt{E_g E_{g-1}}$ to $E' = \sqrt{E_{g'} E_{g'-1}}$.

molecules and their width broadens with increasing T through the diffusion coefficient $D(T)$. As E decreases below E_0 , the quasi-elastic peaks of liquid H_2O become larger and narrower by an incoherent component having the width $Q^2 D(T)$ where Q is the momentum transfer. On the other hand, those of liquid D_2O are not observed distinctly at low E below the diffuse Bragg-cut energy ~ 3 meV since the coherent scattering almost vanishes. (b) There are marked inelastic peaks around $E' \sim 5$ and 60 meV for liquid H_2O and $E' \sim 5$ and 40 meV for liquid D_2O . They represent up-scattering processes ($E' > E$) due to the de-excitations of intermolecular vibration and hindered rotation. Hence, as T increases, they tend to be more significant. (c) For $E > 1$ eV, the recoil scattering in free atoms H, D and O becomes dominant, though it is not clearly seen from Figs. 2 and 3.

Since various properties of neutron scattering in each liquid have been fully discussed in the previous papers [1,2], two typical results among them are presented in Fig. 4 to show essential behavior of the present multigroup constants. The double-differential scattering cross section with the energy change from g to g' is calculated as

$$\frac{1}{(E_{g-1} - E_g)(E_{g'-1} - E_{g'})} \int_{E_g}^{E_{g-1}} dE \\ \times \int_{E_{g'}}^{E_{g'-1}} dE' \frac{d^2 \sigma_s^X(E \rightarrow E', \theta)}{d\Omega dE'}$$

$$= \frac{1}{E_{g'-1} - E_{g'}} \sum_{l=0}^L \frac{2l+1}{4\pi} \sigma_{s,g \rightarrow g'}^{l,X} P_l(\cos \theta). \quad (4)$$

The results of liquid H_2O at 26°C for 304 meV neutrons and liquid D_2O at 26°C for 213 meV neutrons are compared with the experiments [14,15]. It can be seen from Fig. 4 that major behavior of quasi- and inelastic-scattering is well reproduced over the energy range of scattered neutrons at each scattering angle.

The change of neutron energy from E to E' may be simply characterized by the ratio of an averaged energy of scattered neutrons to an incident one. It is defined by

$$\frac{\overline{E}_{f,g}^X}{\overline{E}_g} = \frac{1}{\overline{E}_g \sigma_{s,g}^X} \sum_{g'=1}^G \sigma_{s,g \rightarrow g'}^{0,X} \overline{E}_{g'} \quad (5)$$

where $\overline{E}_g = \sqrt{E_g E_{g-1}}$. Fig. 5 shows the ratios for liquid H_2O and D_2O at four temperatures. It is obvious that there are transition energies of about 40 meV from energy loss ($E' < E$) to gain ($E' > E$) by single scattering. At higher temperature, energy-gain scattering become much significant. The liquid D_2O indicates slightly suppressed ratios around 5 meV on account of inherent coherent scattering.

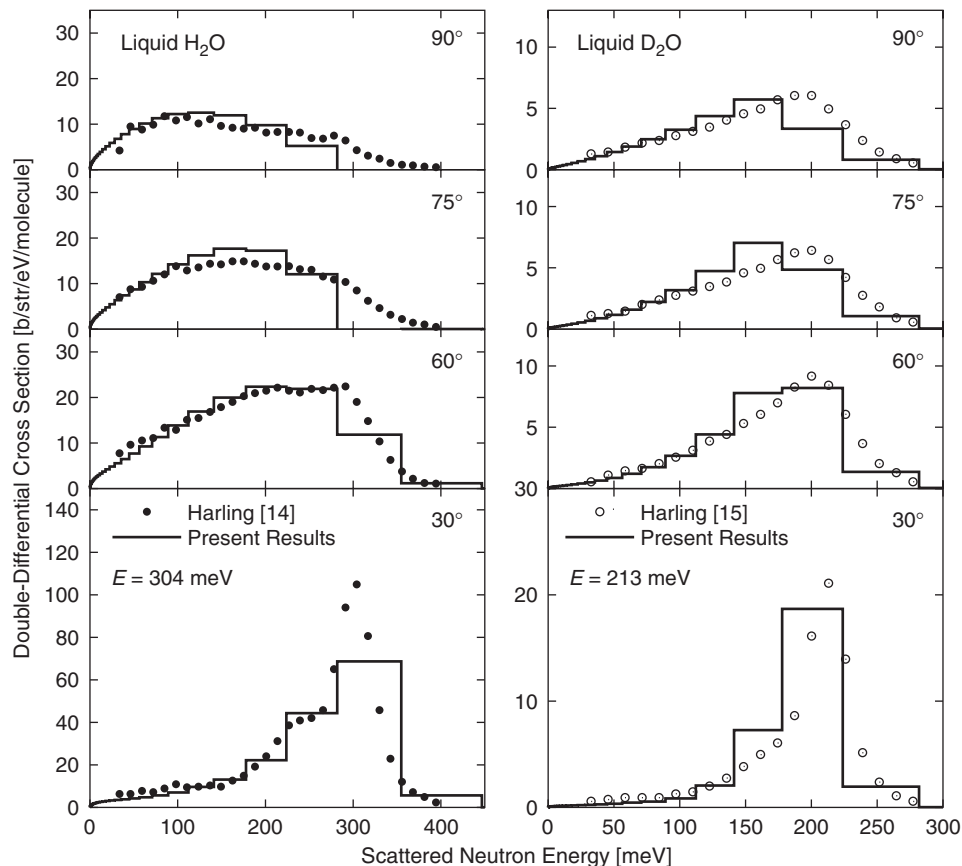


Fig. 4. Double-differential cross sections of liquid H_2O for $E = 304$ meV and liquid D_2O for $E = 213$ meV, together with the experimental results [14,15].

3.2. Angular distributions of scattered neutrons

Angular distribution of scattered neutrons may be evaluated as:

$$f_g^X(\theta) = \frac{1}{\sigma_{s,g}^X} \sum_{g'=1}^G \sum_{l=0}^L \frac{2l+1}{4\pi} \sigma_{s,g \rightarrow g'}^{l,X} P_l(\cos\theta). \quad (6)$$

Since $\int f_g^X(\theta) d\Omega = 1$, then the first moment of $\cos\theta$ is given by

$$\bar{\mu}_g^X = \frac{1}{\sigma_{s,g}^X} \sum_{g'=1}^G \sigma_{s,g \rightarrow g'}^{1,X}. \quad (7)$$

Fig. 6 shows $f_g^{\text{H}_2\text{O}}(\theta)$ and $f_g^{\text{D}_2\text{O}}(\theta)$ as a function of E ($10^{-4} \leq E \leq 10^4$ meV) and θ at 5°C only because their temperature dependence is not significant. For reference, two typical cases of $f_g^{\text{H}_2\text{O}}(\theta)$ with $E = 850$ meV and $f_g^{\text{D}_2\text{O}}(\theta)$ with $E = 6.3$ meV are calculated. The results are compared in Fig. 7 with the experiments [27]. Note that $f_g^{\text{H}_2\text{O}}(\theta)$ for

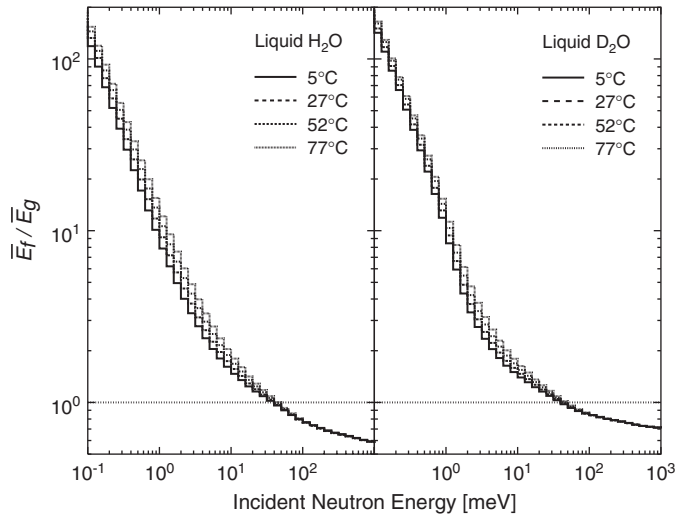


Fig. 5. Ratios of averaged energy of scattered neutrons to incident one.

$E = 20$ meV has been presented in previous paper [1]. Furthermore, Fig. 8 shows the calculated $\bar{\mu}_g^{\text{H}_2\text{O}}$ and $\bar{\mu}_g^{\text{D}_2\text{O}}$ at each temperature, together with the experimental results [17,28]. As a result, the following characteristics may be noted. (a) For liquid H_2O , there is a gradual transition from almost isotropic to distinct forward scattering with increasing E . And (b), for liquid D_2O , an anisotropic behavior due to the diffuse Bragg coherent scattering around 2 meV is obvious. Forward scattering at higher E is relatively weak since $\bar{\mu}_g^{\text{D}_2\text{O}} \sim 0.22$ for $E > 1$ eV.

3.3. Total scattering cross sections

Fig. 9 shows $\Sigma_{t,g}^{\text{H}_2\text{O}}$ and $\Sigma_{t,g}^{\text{D}_2\text{O}}$ at each temperature for neutron energies ranging from 0.1 μeV to 10 MeV, together with $\Sigma_{a,g}^{\text{H}_2\text{O}}$ and $\Sigma_{a,g}^{\text{D}_2\text{O}}$ at lower energies. Compared with the experiments [19,26], the present results demonstrate close agreement over the range from very-cold to epi-thermal neutron energies. Since total cross sections at E higher than

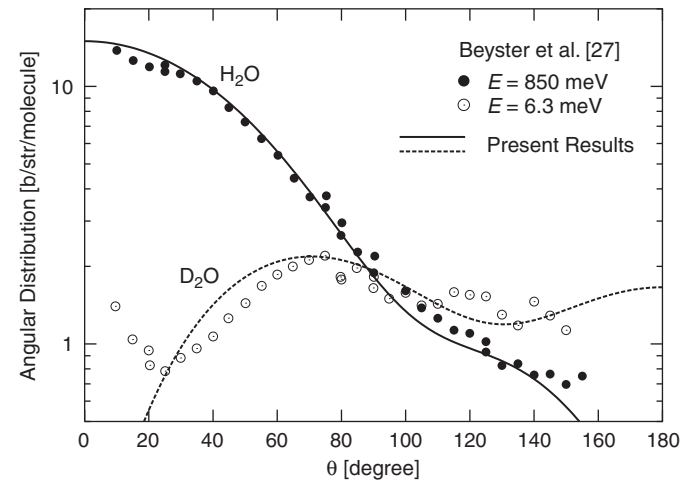


Fig. 7. Angular distributions of liquid H_2O for $E = 850$ meV and liquid D_2O for $E = 6.3$ meV, together with the experimental results [27].

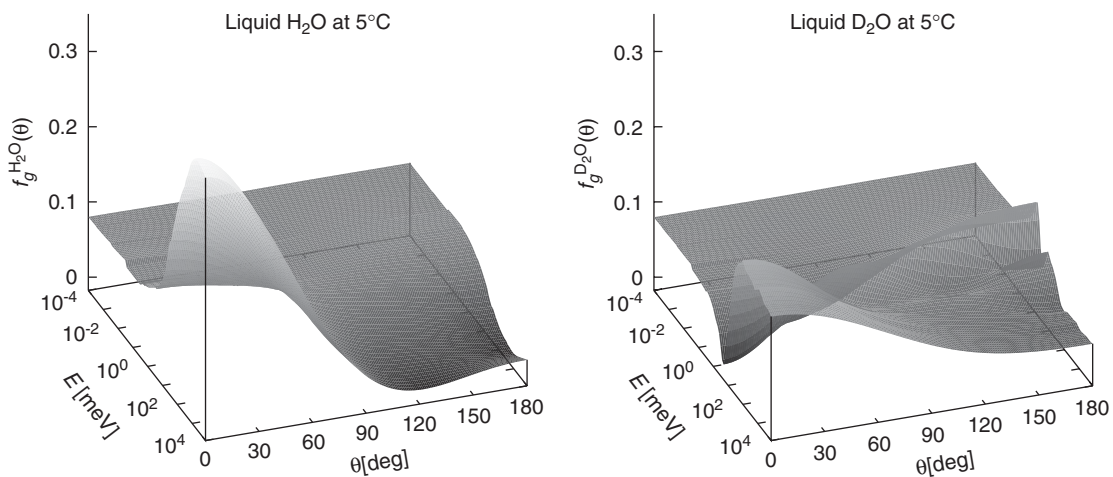


Fig. 6. Angular distributions of scattered neutrons by $f_g^{\text{H}_2\text{O}}(\theta)$ and $f_g^{\text{D}_2\text{O}}(\theta)$.

10 eV have been well-established as an evaluated nuclear data [19,32], only the calculation is presented. The experimental results of liquid D₂O for very-cold neutrons are compared with $\Sigma_{t,g}^{D_2O}$ for pure liquid D₂O and a liquid mixture of 93% D₂O and 7% H₂O. The latter is shown in the insert of Fig. 9 and found to be nearly consistent with the experiments in terms of magnitudes and slopes with a variation in liquid temperature. It may be noted that the Honeck's model [22] for pure D₂O gas at 27°C passes through the experimental very-cold neutron results of liquid D₂O at 23°C though the Nelkin's one [21] for H₂O gas at 27°C largely over-estimates the relevant experiment. Consequently, the present multigroup constants based on the liquid water models are found to be adequate over the wide energy range concerned with, say, very-cold to fast

neutrons. Finally, it is further mentioned that the diffuse Bragg coherent scattering in liquid D₂O is well reproduced around 3 meV and that gradual transitions of $\sigma_{t,g}^{H_2O}$ and $\sigma_{t,g}^{D_2O}$ to respective free atom cross section, i.e. 44.6 b and 10.6 b for $E \sim 10$ eV, can be ascertained.

Following the argument in Ref. [26], the calculated total cross sections at very-cold neutron energies are characterized as follows. A linear function of a neutron wavelength $\lambda_g (\propto 1/\sqrt{E_g})$, $m(T)\lambda_g + c(T)$, is fitted to $\Sigma_{t,g}^{H_2O}$ and $\Sigma_{t,g}^{D_2O}$, so that the magnitudes of $m(T)$ as well as $c(T)$ are determined at each temperature. The fitting region is selected to be $0.0021 < E < 0.053$ meV and the average deviation is less than 0.3%. Fig. 10 shows the values of $m(T)$ for liquid H₂O and D₂O as a function of temperature. Also shown in Fig. 10 are the experimental and theoretical results taken from Ref. [26]. The present results of liquid H₂O exhibit an increasing tendency of $m(T)$ with temperature, while those of liquid D₂O are rather gradual on account of less magnitude of $\Sigma_{t,g}^{D_2O}$. Such tendencies may be explained physically by reference to the results of Figs. 2 and 3. At lower temperatures, the quasi-elastic scattering by molecular diffusion is relatively significant, whereas it becomes less effective with increasing T by the enhancement of up-scattering due to the de-excitations of intermolecular vibration and hindered rotation. These temperature-dependent processes of liquid dynamics have been included in the multigroup constants through the cross section model of liquid H₂O and D₂O [1,2], which is essentially in contrast with the models of Nelkin [21], Debye crystal [33], simple self-diffusion [33] and Esch [34].

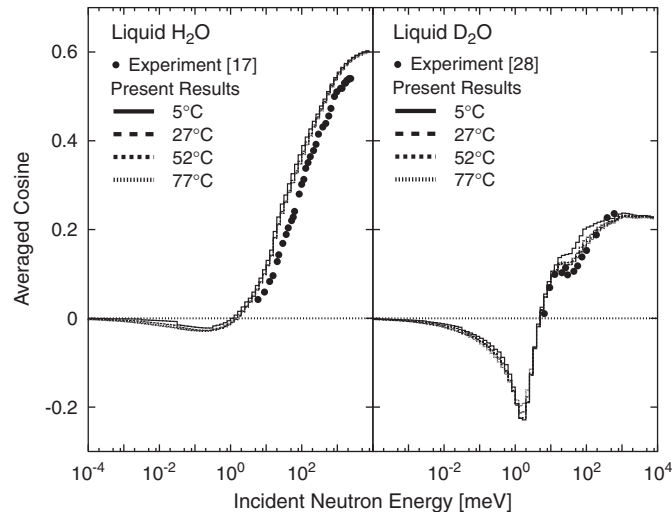


Fig. 8. Averaged cosines of scattered neutrons by $\bar{\mu}_g^{H_2O}$ and $\bar{\mu}_g^{D_2O}$, together with the experimental results [17,28].

3.4. Integral tests with neutron energy spectra

As an integral test of the multigroup constants, they are applied to the neutron transport analysis of large homo-

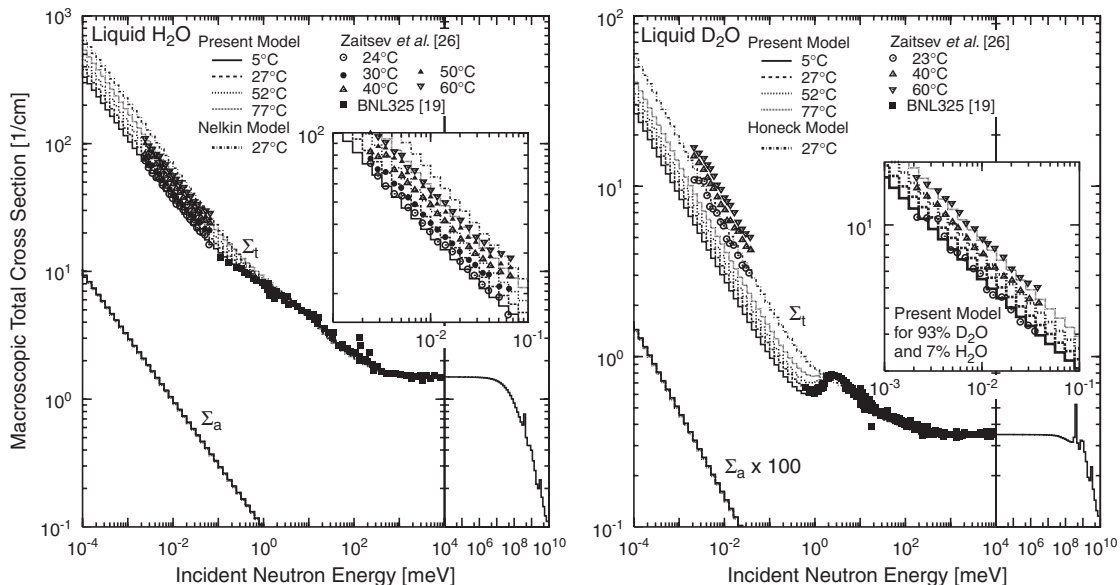


Fig. 9. Macroscopic total and absorption cross sections, $\Sigma_{t,g}^X$ and $\Sigma_{a,g}^X$, for liquid H₂O and D₂O, together with the experimental results [26,19].

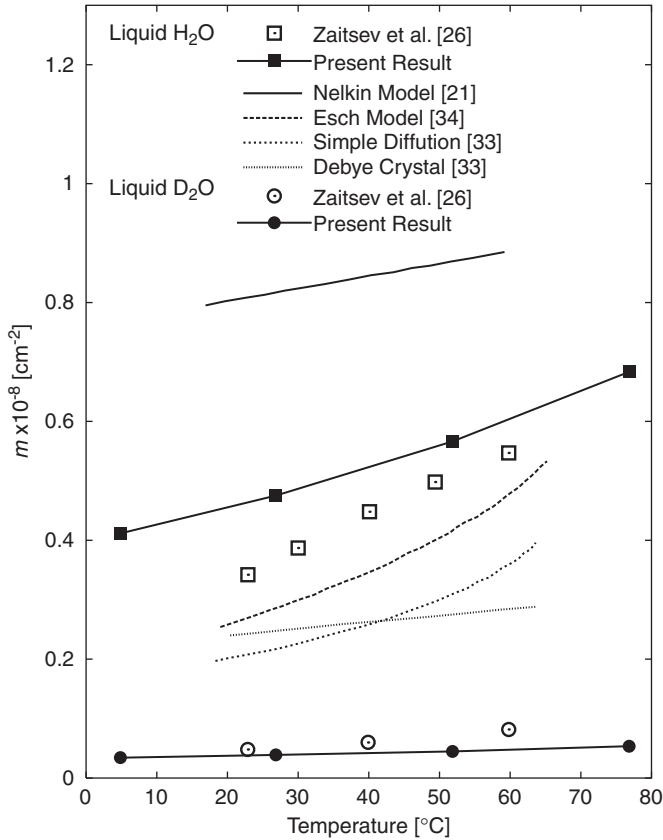


Fig. 10. Temperature dependence of the slope $m(T)$ for liquid H_2O and D_2O , together with the experimental results [26].

geneous moderators composed of liquid H_2O and D_2O . The purpose is to make sure of the reproduction of equilibrium energy spectra of neutron flux inherent to each liquid. Hence infinite-medium spectra are calculated under the condition of a spatially uniform external source of fission neutrons with an average energy of ~ 2 MeV. A neutron transport code ANISN [35] in the P_3 - S_8 approximation is used. A set of energy spectra for pure liquid H_2O and D_2O at 27°C , together with mixtures of them and liquid H_2O poisoned with $\sqrt{E_0/E}$ absorber, are calculated. Fig. 11 shows the calculated results for the whole neutron energies from $0.1 \mu\text{eV}$ to 10 MeV. In addition, the spectra measured in liquid H_2O and poisoned water [29] are presented since they can be considered infinite medium spectrum [36,37]. To characterize the energy spectra of thermal neutrons, the following expression in a Maxwellian plus $1/E$ form [38] is fitted by a least-square method:

$$\phi(E) dE = \phi_{\text{M.B.}}(E) dE + \Delta(E) \phi_{\text{S.D.}}(E) dE \quad (8)$$

where

$$\phi_{\text{M.B.}}(E) dE = \phi_{\text{th}} \frac{E}{(k_{\text{B}} T_{\text{n}})^2} \exp\left(-\frac{E}{k_{\text{B}} T_{\text{n}}}\right) dE \quad (9)$$

$$\phi_{\text{S.D.}}(E) dE = \phi_{\text{epi}} \frac{1}{E} dE \quad (10)$$

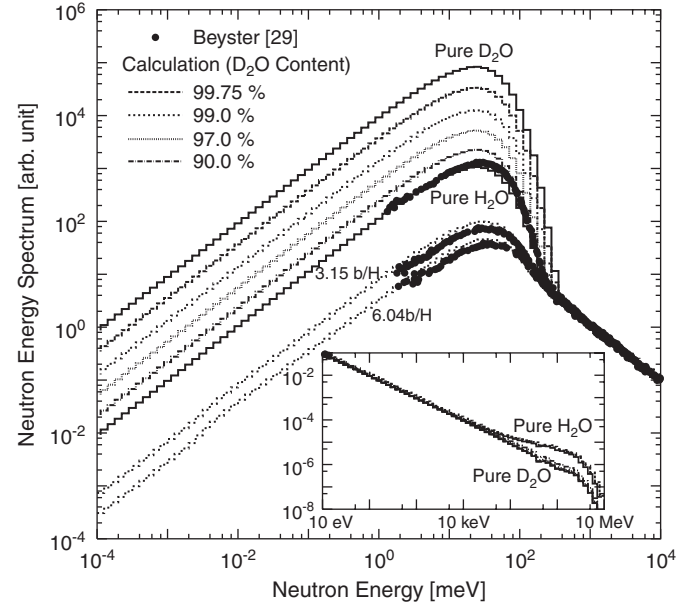


Fig. 11. Infinite-medium energy spectra of neutron flux for liquid H_2O and D_2O at 27°C , normalized to the $1/E$ component above 0.5 eV.

$$\Delta(E) = \begin{cases} \frac{2}{1 + \exp(A/\sqrt{E-B})}, & (E > B) \\ 0, & (E \leq B) \end{cases} \quad (11)$$

ϕ_{th} is the total flux of thermal neutrons, T_{n} is the effective neutron temperature, k_{B} is the Boltzmann constant, ϕ_{epi} is the epi-thermal neutron flux, A and B are the fitting free parameters. Fig. 12 shows the resulting values of $(T_{\text{n}} - T)/T$ and $\phi_{\text{th}}/\phi_{\text{epi}}$ for pure liquid H_2O and D_2O and mixtures of them at each temperature. The following moderating properties can be ascertained from Figs. 11 and 12: (a) good moderation to thermal neutrons is attained in liquid D_2O and liquids rich in D_2O , on account of the very weak absorption of lower-energy neutrons and the lower excitation energy of hindered rotation. (b) Spectral indexes of $(T_{\text{n}} - T)/T$ and $\phi_{\text{th}}/\phi_{\text{epi}}$ indicate slight temperature dependence. In particular, as T increase, $\phi_{\text{th}}/\phi_{\text{epi}}$ for pure liquid H_2O and D_2O approaches the theoretical value of moderating ratio, given by 71 and 5700, respectively [38].

A further study of the infinite-medium spectra $\Phi(E)$ is pursued on the question whether fine structure due to the molecular dynamics is found or not. A relative deviation of $\Phi(E)$ from the fitted $\phi_{\text{M.B.}}(E)$ is defined as $\Phi(E)/\phi_{\text{M.B.}}(E) - 1$ and calculated for pure liquid H_2O and D_2O at each temperature. Fig. 13 shows the percent deviations for neutron energies between 0.1 and 100 meV, compared with those by Nelkin model for liquid H_2O [21] and Honeck model for liquid D_2O [22]. Non-Maxwellian deviations are obvious, which arise mainly from two up-scattering processes by the de-excitations of intermolecular vibration and hindered rotation: their respective energy gains are about 5 and 60 meV for liquid H_2O and about 5 and 40 meV for liquid D_2O . At lower temperatures, the peak width of such scattering is relatively narrow (see Figs. 2

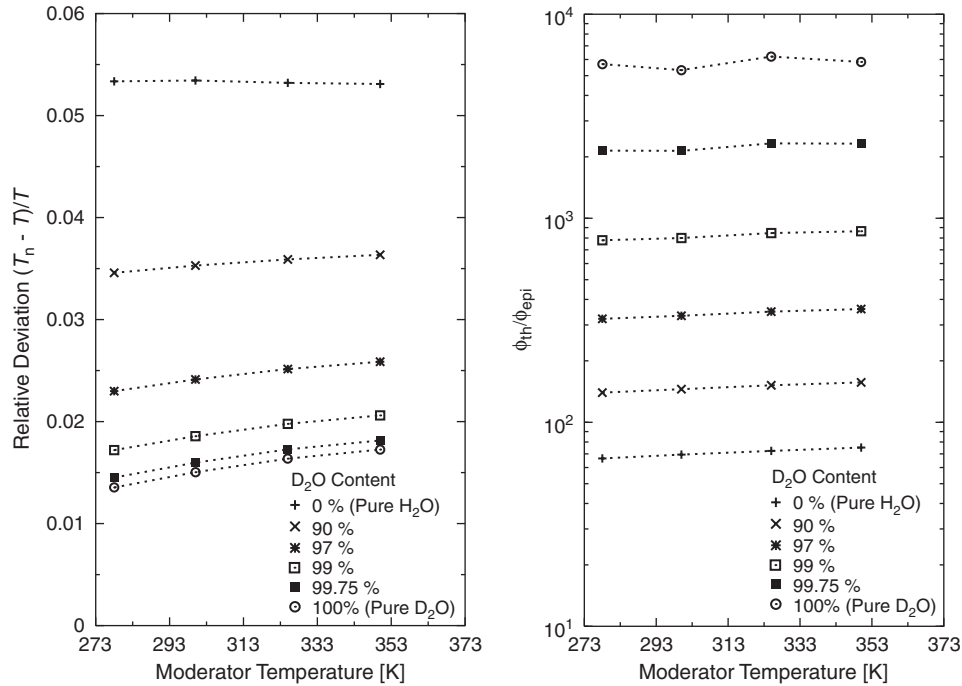


Fig. 12. Temperature dependence of neutron temperature deviation $(T_n - T)/T$ and moderating ratio ϕ_{th}/ϕ_{epi} .

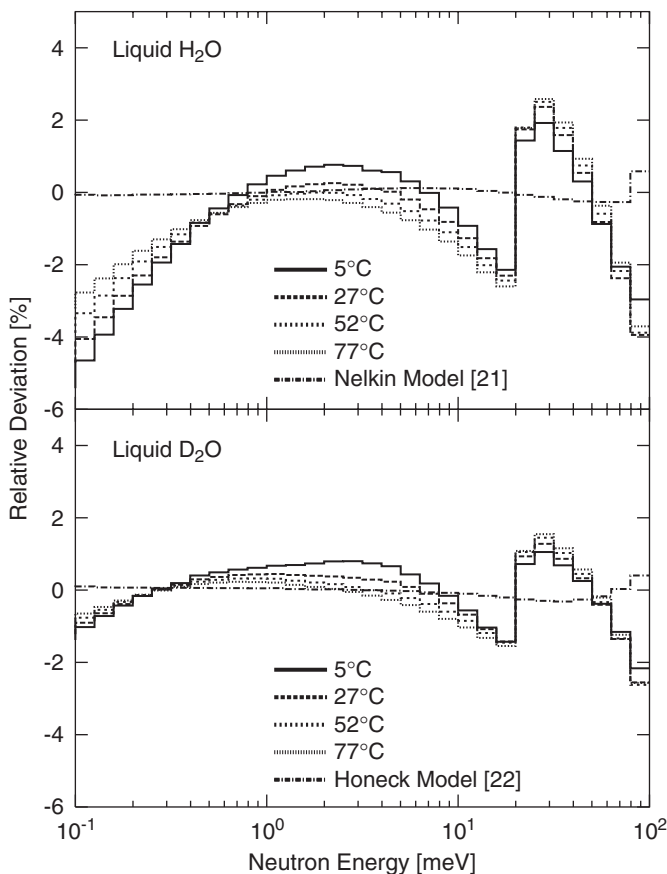


Fig. 13. Relative deviations of the calculated spectra from the fitted Maxwellian one at the temperatures shown, compared with those by the Nelkin model [21] and Honeck model [22].

and 3), thus resulting in up-scattering with specific energy gains. As liquid temperature is raised, the peaking behavior becomes more marked with both increased magnitude and broad tail component. The former enhances the deviations around 30 meV and the latter moderates the ones below about 10 meV. In the case where such an up-scattering accompanied with specific energy gains is not significant, the condition of detailed balance tends to be satisfied. This extreme is illustrated with the almost Maxwellian behavior of the Nelkin and Honeck models since they are essentially molecular-gas models for translational motion.

4. Concluding remarks

The eight sets of multigroup constants for liquid H₂O and D₂O at 5, 27, 52 and 77 °C have been successfully generated, which are examined for physical and quantitative characteristics:

- A wide range of neutron energies from 0.1 μeV to 10 MeV is covered so that slowing-down and thermalization of spallation/fission neutrons to ultra-cold ones can be analyzed as a whole.
- Scattering properties of liquid water are fully included, thus resulting in good reproduction of scattering laws [14–16,20], double-differential cross sections [14,15], angular distributions [27,17,28] and total cross sections [26,19]. This essentially contrasts with the results of ordinarily used models such as Nelkin [21] and Honeck [22].

- Integral tests with infinite-medium energy spectra for thermal neutrons reveal that the effects of water molecular dynamics and H₂O/D₂O content are significantly dependent on liquid temperature.

Consequently it may be concluded that, in combination with the already developed multigroup constants for liquid H₂ and D₂, solid and liquid CH₄ and super-fluid ⁴He [23–25], the present ones are expected to serve for development of an advanced neutron source to be installed at a high-power proton accelerator and a high-flux research reactor.

Acknowledgments

The authors are grateful to Dr. S.P. Kuznetsov of the Lebedev Physical Institute for informing us of the experimental results [26] with valuable comments. Drs. S. Tasaki and Y. Abe are acknowledged for useful discussions.

References

- [1] Y. Edura, N. Morishima, Nucl. Instr. and Meth. A 534 (3) (2004) 531.
- [2] Y. Edura, N. Morishima, Nucl. Instr. and Meth. A 545/1–2 (2005) 309.
- [3] Y. Edura, N. Morishima, Physica B 350 (1–3, Suppl. 1) (2004) E655.
- [4] Y. Edura, S. Tasaki, N. Morishima, Cross section model and scattering law of liquid water for design of a cold neutron source, in: Proceedings of the 2003 Symposium on Nuclear Data, vol. JAERI-Conf. 2004–2005, Tokai, Japan, 2004, pp. 242–247.
- [5] G.H. Vineyard, Phys. Rev. 110 (5) (1958) 999.
- [6] G. Palinkas, E. Kalman, P. Kovacs, Mol. Phys. 34 (2) (1977) 525.
- [7] J. Teixeira, M.-C. Bellissent-Funel, S.H. Chen, A.J. Dianoux, Phys. Rev. A 31 (3) (1985) 1913.
- [8] F. Cavatorta, A. Deriu, D.D. Cola, H.D. Middendorf, J. Phys.: Condens. Matter 6 (23A) (1994) A113.
- [9] G.C. Lie, E. Clementi, Phys. Rev. A 33 (4) (1986) 2679.
- [10] G. Corongiu, E. Clementi, J. Chem. Phys. 98 (6) (1993) 4984.
- [11] P.V. Blanckenhagen, Ber. Bunsenges. für Phys. Chem. 76 (9) (1972) 891.
- [12] M.-C. Bellissent-Funel, S.H. Chen, J.-M. Zanotti, Phys. Rev. E 51 (5) (1995) 4558.
- [13] M. Sakamoto, B.N. Brockhouse, R.G. Johnson, N.K. Pope, J. Phys. Soc. Jpn. 17 (Suppl. B-II) (1962) 370.
- [14] O.K. Harling, J. Chem. Phys. 50 (12) (1969) 5279.
- [15] O.K. Harling, Nucl. Sci. Eng. 33 (1968) 41.
- [16] B.C. Haywood, J. Nucl. Energy 21 (1967) 249.
- [17] J.R. Beyster, Nucl. Sci. Eng. 31 (1968) 254.
- [18] V.H.-D. Lemmel, Nukleonik 7 (1965) 265.
- [19] D.I. Garber, R.R. Kinsey, Neutron cross sections BNL-325 volume II, curves, Technical Report BNL-325, Brookhaven National Laboratory, 1976.
- [20] B.C. Haywood, D.I. Page, The scattering law for heavy water at 540°K and light water at 550°K, in: IAEA Symposium on Neutron Thermalization and Reactor Spectra, International Atomic Energy Agency, Vienna, 1967, p. 17.
- [21] M. Nelkin, Phys. Rev. 119 (2) (1960) 741.
- [22] H.C. Honeck, Trans. Am. Nucl. Soc. 5 (1962) 47.
- [23] N. Morishima, Y. Matsuo, Nucl. Instr. and Meth. A 490 (1–2) (2002) 308.
- [24] Y. Sakurai, T. Mitsuyasu, N. Morishima, Nucl. Instr. and Meth. A 506 (1–2) (2003) 199.
- [25] Y. Abe, N. Morishima, Nucl. Instr. and Meth. A 481 (1–3) (2002) 414.
- [26] K.N. Zaitsev, V.N. Petrov, S.P. Kuznetsov, O.A. Langer, I.V. Meshkov, A.D. Perekrstenko, Atomnaya Énergiya 70 (3) (1991) 184.
- [27] J.R. Beyster, J.M. Neill, J.C. Young, Recent developments in integral neutron thermalization, in: Reactor Physics in the Resonance and Thermal Regions, Neutron Thermalization, vol. I, MIT Press, Cambridge, MA, 1966, pp. 151–193.
- [28] J.R. Beyster, General atomic report, Technical Report GA-6824, 1965.
- [29] J.R. Beyster, Nucl. Sci. Eng. 9 (2) (1961) 168.
- [30] N. Morishima, J. Neutron Res. 13(4) (2005) 225.
- [31] E. Lemmon, M. McLinden, D. Friend, Thermophysical properties of fluid systems, in: NIST Chemistry WebBook, NIST Standard Reference Database Number 69, National Institute of Standards and Technology, Gaithersburg, MD, 20899, 2003. URL: <http://webbook.nist.gov>
- [32] P.F. Rose (Ed.), Cross section evaluation working group, ENDF-201 ENDF/B-VI summary documentation, Technical Report BNL-NCS-17541, National Nuclear Data Center, Brookhaven National Laboratory, Upton, NY, USA, 1991.
- [33] K. Binder, Wirkungsquerschnitte für die streuung von ultrakalten neutronen (interaction cross sections of the scattering of ultracold neutrons), PTHM-FRM-110, 1970.
- [34] L. Esch, M. Yeater, W. Moore, K. Seemann, Nucl. Sci. Eng. 46 (1971) 223.
- [35] W. Engle, Jr., A user's manual for ANISN: a one-dimensional discrete ordinates transport code with anisotropic scattering, Technical Report K-1693, Oak Ridge Gaseous Diffusion Plant, Tennessee, 1967.
- [36] K. Beckurts, K. Wirtz, Neutron Physics, Springer, 1964.
- [37] V. Turchin, Slow Neutrons, Jerusalem: Israel Program for Scientific Translations, 1965.
- [38] J.M. Carpenter, W.B. Yelon, Neutron sources, in: Methods of Experimental Physics, Neutron Scattering, vol. 23, Academic Press, Orlando, FL, 1986, pp. 99–196.